IEEE Access
Multidisciplinary | Rapid Review | Open Access Journal

Received January 27, 2021, accepted February 28, 2021, date of publication March 8, 2021, date of current version March 18, 2021.

Digital Object Identifier 10.1109/ACCESS.2021.3064347

Diagnosis of Inter-Turn Shorts of Loaded Transformer Under Various Load Currents and Power Factors; Impulse Voltage-Based Frequency Response Approach

NATARAJAN SHANMUGAM[1], SRINIVASAN GOPAL[2], BALASUBRAMANIAN MADANMOHAN[1], (Member, IEEE), S. P. BALAJI[3], (Member, IEEE), AND RAJESH RAJAMANI[1]

[1]Department of Electrical and Electronics Engineering, Shanmugha Arts, Science, Technology and Research Academy (SASTRA) Deemed University, Thanjavur 613401, India
[2]W.S. Test Systems, Bengaluru 562157, India
[3]Global Power Research Institute (GPRI), Cuddalore 607302, India

Corresponding author: Natarajan Shanmugam (natarajans@eee.sastra.edu)

The authors thank SASTRA Deemed University and DST-FIST (: SR/FST/ETI-338/2013(C) dated 10/09/2014) for their motivation.

ABSTRACT Inter-turn short circuits within the transformer winding are diagnosable through the impulse voltage based frequency response analysis (IFRA). If the diagnosis is made Online, interruption to the power network can be avoided. However, the transformer's load may influence the frequency response based diagnostic process, and this aspect has not yet been investigated. Motivated by this research gap, experimental investigations were carried out on a three-phase 5 kVA, 440 V/440 V Star/Delta transformer and a three-phase 315 kVA, 11 kV/433 V, Dyn11 distribution transformer, when they were supplying power to loads of different magnitudes and power factors. The influence of the load current and its power factor on the IFRA was observed under the transformer's healthy condition and with inter-turn short circuits in one of the windings. Investigations under these different loaded conditions revealed that a signature FRA plot developed at a particular load condition cannot be directly used for assessing the condition of the transformer at a different load. Both the magnitude and the power factor of the load are found to influence the frequency response. A careful interpretation of the Frequency response of the transformer, based on its load, was found effective in detecting and locating the inter-turn shorts.

INDEX TERMS Frequency response analysis, transformer, inter-turn shorts, diagnosis, transfer function, statistical tools, online diagnosis.

I. INTRODUCTION

The transformer is a vital component in any power system network, and its condition must be ensured good for the reliable operation of the network. Several faults can develop within the transformer due to various stresses imposed on them, right from their manufacturing period, transportation, commissioning upto their continuous service period. Such faults are diagnosed by conducting various tests like the insulation resistance measurement, ratio test, open and short circuit tests, dissolved gas analysis of transformer oil, power frequency and impulse voltage tests, partial discharge tests, separate source and induced overvoltage tests, frequency response analysis etc. They are explained in various standards and various literature [1]–[4].

Frequency Response Analysis (FRA) is evolving as a user-friendly technique and preferred for the diagnosis of the mechanical deformations within the transformer winding, inter-turn shorts, core magnetization problems and, various issues arising out during transportations and poor grounding connections [5]–[10]. Based on the type of the test signal (usually referred as the Input or the Excitation signal), they can be done in two ways: (i) Sweep Frequency Response Analysis (SFRA) and (ii) Impulse voltage based Frequency

The associate editor coordinating the review of this manuscript and approving it for publication was Zhixiong Peter Li.

Response Analysis (IFRA). SFRA uses a sweep sinusoidal signal of constant magnitude as the test signal, which is covering for a wide frequency range (Hz-MHz) [11]. IFRA uses a single impulse voltage as the test signal, which can be viewed to be made up of the superposition of several sinusoidal signals of different frequencies and magnitudes, thereby covering a wide frequency range as per the concept of the Fast Fourier Transform (FFT) [11]. Standards, Working Group recommendations and Guidelines are available for conducting the SFRA as an Offline which are explaining the FRA test circuitry, various test procedures and offer guidelines for the interpretation of the FRA results for the diagnosis of the mechanical displacements within the transformer [12]–[14]. Several researchers have successfully used these guidelines for both the SFRA and IFRA and demonstrated their effectiveness in the diagnosis of mechanical displacements as well as other faults like the inter-turn- shorts within the windings and the magnetic core issues [11]. Literature also reports in detail, the various factors that can influence the FRA test results and recommend the various standard procedures to be followed for ensuring the reliability of the FRA results [12]–[14]. FRA plots were usually referred as Transfer Function (TF) plots and, were found to be useful in indicating the presence of the faults within the transformer in the form of the changes in the transfer function plots such as the appearance of new spikes and dips, the disappearance of the existing spikes and dips, changes in the dB magnitudes [8]–[10]. However, the interpretation of such results invites experience or expert service. Various tools like support vector machines, wavelets and other soft computing techniques for the analysis of the FRA results were reported in the literature [15]–[19]. The usefulness of various statistical parameters in reducing the interpretation difficulties of the FRA results was demonstrated in various works [20]–[22]. However, most of these FRA works were done as Off-line diagnosis, by taking the transformer out of service, from the power system network [23]–[25].

If FRA is carried out on the transformer as an Online diagnosis, any power system outages required for assessing the condition of the transformers can be avoided, which can increase the reliability of power system network, as a whole [27]. Off-line and Online FRA works were compared by some researchers, and the current and future trends of the FRA works were briefed by some researchers [26], [27]. Only a very few works are available on the Online implementation of FRA, as simulations and real-time experimental works [28]–[31]. Difficulties in the test signal injection into the transformer when it is On-line was given the main focus and addressed in detail in such works, which are highly motivating. In the previous works of the authors, some experimental works done with the Online On-load IFRA (OLOL IFRA) approaches were explained, and the focus was given to the methodology of OLOL IFRA implementation, isolation requirements within the setup between the Impulse signal source and the power supply source and the usefulness of statistical tools in the interpretation of the FRA results [32].

The influence of the load on the diagnosing capability of IFRA has not been given much attention in the previous works. Loads connected to the transformer can alter the overall impedance imposed on the IFRA test circuitry and, thus, can challenge the effectiveness of the diagnostic process. Motivated by this research gap, an experimental investigation was carried out by the authors on a three-phase, 5 kVA, 440 V/ 440 V, star/ Delta transformer and a three-phase, 315 kVA, 11 kV/ 433 V, Dyn11, distribution transformer. With a variable three-phase load bank connected to the transformers, inter-turn short circuits were emulated in the transformer windings. The diagnosis of such emulated short circuits in the transformers under different loaded conditions was, carried out with the IFRA approach.

The main focus of the present work was on the effect of (i) transformers' load magnitude and (ii) its power factor, on the IFRA result. For this purpose, different load conditions were considered, with the load current at different magnitudes and different power factors (Unity, lagging and leading). The frequency responses of the transformer winding were observed, both under its healthy condition ('No-fault' case) and faulty condition (with the 'inter-turn' shorts).

Differences observed in the End-to-End voltage transfer function plots, and the statistical parameters extracted from the transfer function data have indicated that both the Load (current magnitude) and its type (Power factor of the load) can influence the frequency response of the transformers. The present work becomes significant as it demonstrates the need for the careful interpretation of the FRA results based on the load parameters, during the inter-turn short diagnosis and thus addresses an important research gap in the Online IFRA approach.

For making the work reproducible, the details of the test specimen, the various cases investigated, and the procedures followed for experimentation and analysis of the results were presented in the methodology section. In the Results and discussion section, the effect of load parameters on the efficacy of IFRA was discussed, based on the results of the various investigations. Finally, in the conclusion section, the insights got on the influence of the load parameters on the IFRA were presented. The investigations demonstrated that the challenges imposed by the load parameters on the Online IFRA could be tackled effectively by taking into account the loading effects in the signature IFRA pattern itself.

II. METHODOLOGY

Experimental investigations were carried out on two transformers, for analyzing the impact of load magnitudes and their power factors on the diagnosing capability of the Online IFRA.

As a first specimen, a 3 phase 5 kVA, 440 V/440 V Dyn 11 transformers with tappings at 0 V, 30 V, 115 V, 230 V and 440 V levels in the Star side was used. A balanced three-phase, 50 Hz supply was given to the star side. For loading the transformer to different current magnitudes and power factor, the delta side of the transformer was connected to a

variable loading arrangement comprising of a parallel combination of loading rheostat, inductive load and a capacitive bank. By switching them in different combinations, three different levels of loadings were achieved at 4 A load level; (1) Unity power factor (UPF),(2) 0.5 PF Lagging and (3) 0.5 PF Leading.

As a second specimen, a 3 phase 315 kVA, 11 kV/ 433 V, Dyn 11 Distribution transformer was used. This transformer has specially created tappings at 87.5%, 62.5%, 37.5%, and 12.5% positions along the R–phase winding (1U-1V), referred from the (1V) toward (1V) on the delta side. As shown in Figure 1, the terminals (1U), tappings at 87.5%, 62.5%, 37.5%, and 12.5% levels and the terminal (1V) are referred as t1, t2, t3, t4, t5 and t6 respectively. As this second specimen was currently under use for different research works, IFRA tests were conducted at reduced voltage levels only so that no permanent damage was caused to the transformer during the investigations. Irrespective of the supply voltage magnitude, the inter-turn shorts offer the same ohmic loading on the transformer. Hence, during the present investigation, a balanced three-phase, 50 Hz, low-voltage, alternating supply was given on the star side. The objective of the work was to analyze the influence of the load current magnitude and its power factor on the fault diagnosing capability of IFRA. A variable loading arrangement was connected to the delta side, for achieving different loading conditions at different power factors; (1) with a load current of 10 A at UPF, 0.94 PF lagging and 0.94 PF leading and, (2) with a load current of 11 A at UPF,0.85 PF. lagging and 0.85 PF leading.

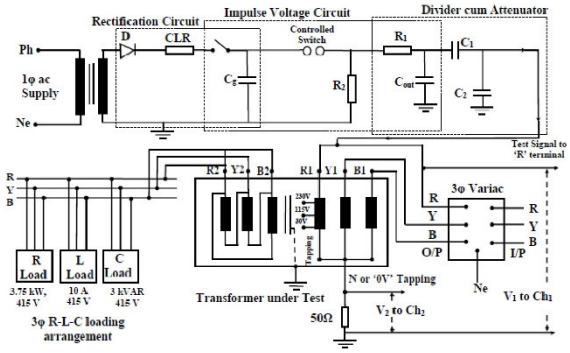

FIGURE 1. Experimental circuitry for the IFRA investigation on the 5 kVA transformer.

A. EXPERIMENTAL SETUP

Figure 1 shows the experimental setup for 5 kVA transformer specimen, and figure 2 shows the photograph.

An Impulse generator kit was assembled and used to apply a lightning impulse voltage, as the test signal (referred hereafter as the input or the excitation signal) throughout the IFRA investigation. As the major challenge in Online IFRA implementation is the isolation requirement between the ac source side and the impulse source side, an attenuator was purposefully included between them. The impulse was applied to the

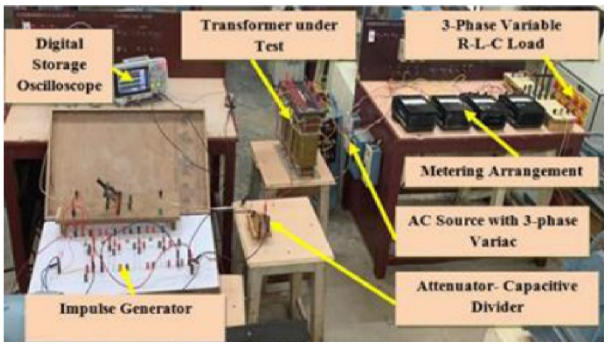

FIGURE 2. Photograph of the Experimental circuitry for 5 kVA transformer.

440 V terminal of the R-phase of the star side, with reference to the ground, through the attenuator circuit. The attenuator is basically a capacitive ladder circuit and thus acts as a high pass filter. The attenuator, thus, offers an easy path for the impulse voltage (comprising of high-frequency components, in the majority) and, a very high ohmic path for the alternating supply, back-flowing from the transformer into the impulse generator. The attenuator offers some loading effect on the test signal and thus distorts its shape by offering different ohmic opposition to the different frequency components of the impulse. IFRA is, basically, in need of a test signal with an appreciable spectrum of frequency and, does not depend much on the shape of the injected signal.

During the IFRA investigation, a Standard LI Voltage signal with a peak value of 380 V was generated from the impulse generator and applied to the transformer through the attenuator circuit. The impulse signal got distorted in its shape and magnitude due to the loading effects. The magnitude of the injected impulse was found to be 80 V, with its frequency contents spanning from 100 Hz to 10 MHz. As the net attenuated impulse signal still contains a good spectrum of high-frequency components of appreciable magnitudes and thus meets out the basic requirement of the Frequency Response Analysis (FRA.) technique, the loading effects of the attenuator during the investigation is acceptable, as referred in various literature [24], [31].

The three-phase alternating voltage supplied to the transformer and the load connected on its delta side are balanced and hence do not engage the ground in its return path. However, the impulse voltage circuitry uses the ground as the return path. For engaging the impulse voltage as the test signal and passing the same into the transformer winding under investigation, the neutral tapping of the transformer's star side was purposefully grounded through a 50 Ω resistor. As shown in Figure 1, the resistor has got included only in the impulse path. The response of the transformer winding to the test impulse voltage thus reaches the resistor. Hence, it can be used to represent the voltage reaching the other end of the tested winding. Thus, a provision for the injection of the impulse into one end of the winding and the measurement of response at the other end of the winding were ensured. These arrangements simultaneously restrict the

engagement of the alternating supply to the transformer side only.

Investigations were carried out with the first transformer (5 kVA) under its healthy condition and, with the fault (emulated inter-turn short circuit between the '0 V' and '30

V' tappings of the R-phase primary winding, through a 500 Ω, 25 W resistor). The resistor was chosen such that it could represent a short at a developing stage (low level) and the current circulating within the shorted portion of the winding could not exceed the rated current level of the winding. Thus, any possible permanent damage to the transformers during the investigations was avoided. Figure 1 shows the experimental setup. Figure 2 shows its photograph.

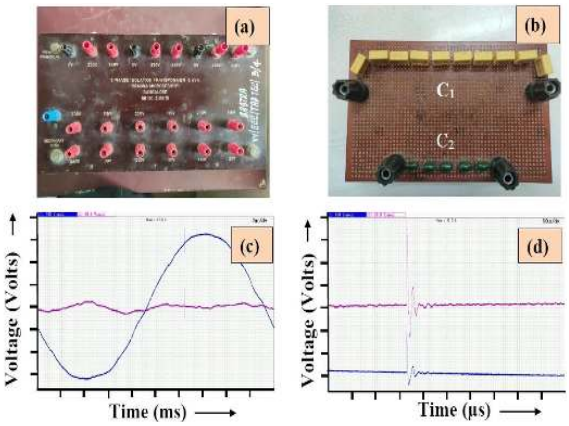

FIGURE 3. Photographs of (a) the transformer terminals, (b) attenuator, (c) end to end voltage waveforms and, (d) the zoomed portion of the waveforms at which the impulse is super-imposed.

Figure 3 shows the transformer terminals, attenuator, end to end voltage waveforms and, the zoomed portion of the waveform at which the impulse got super-imposed on the a.c supply.

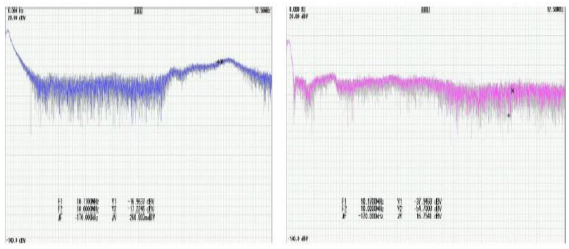

FIGURE 4. FFT plots of Input(V1) and response(V2) voltages.

Figure 4 illustrate the frequency contents with the Input (V1) and response voltages(V2), in terms of their FFT plots.

Throughout the investigation, the impulse voltage injected at the 440 V terminal of the R-phase of the Star side was, considered as the test input signal (V1). The voltage received at the other end of the same winding (neutral (or) 0 V terminal) was viewed as the response Voltage (V2). In the circuit, this voltage was appearing across the grounding resistor (50 Ohm) between the neutral point and the ground. On the Delta side, the three-phase, variable load bank was connected. For measuring the load current magnitude and its power factor, appropriate ammeter and voltmeter and wattmeter were included. The input voltage (V1) and its response (V2) appearing at the two ends of the winding were also referred as the End to End voltages(EEV) and, observed at the Channel-1 and channel-2 of a Digital Storage Oscilloscope (DSO) respectively (Keysight make, 2 GHz, 2 G.sa/sec, 2 Ch) [33].

Though the transformer continuously engages the 50 Hz, ac supply, the trigger control was set for the channel-2 such that, the voltages V1 and V2 were captured in the DSO, only when the impulse voltage was injected to the winding. Figure (3.C) shows the waveforms of V1 and V2, wherein the impulse gets superimposed on the base (50 Hz) sinusoidal voltage at the time of triggering. The magnified version of the portion of the voltages where the impulse gets superimposed was, shown as figure (3.D).

The DSO has an in-built FRA function for getting the FRA data. The FRA plots were developed, by taking (20 $\log_{10}$ (V1/V2)) for the various frequency components of the voltages in Y-axis, against, the corresponding Frequencies in X-axis. These FRA plots were referred to as End-End Voltage Transfer function (EEV TF) plots.

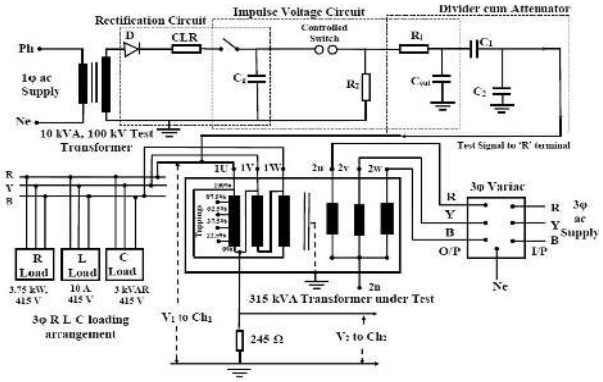

FIGURE 5. Circuit for IFRA investigation of 315 kVA transformer.

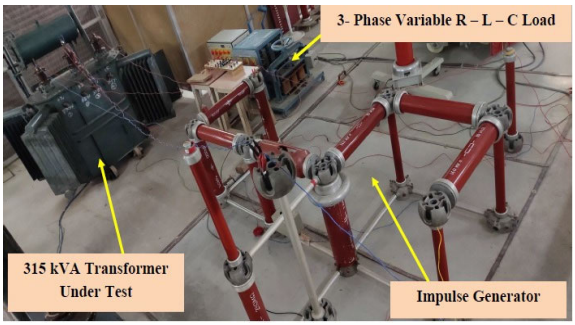

FIGURE 6. Photograph of the Experimental circuitry for 315 kVA transformer.

Figure 5 shows the experimental set of 315 kVA transformer. Figure 6 shows its photograph.

The HV capacitors, diodes and resistors, available at HV lab of SASTRA were used for applying a lightning impulse voltage as the test signal (referred hereafter as the Input). The impulse was applied to the 11 kV terminal of the R-Phase of the delta side, with reference to the ground, through an attenuator circuit comprising of C1 (100 pF and C2 (1200 pF). These high voltage capacitors offered high ohmic

opposition to the back-flowing ac supply and low opposition to the high frequency components of the impulse voltage. The voltage reaching the other terminal (1V) of the R phase winding was, considered as the response voltage (V2). The terminal (1V) of the delta side was, shorted with the (1W) terminal and grounded through a low ohmic resistance (245 Ohm), as per the impulse test procedure.

During the IFRA investigation, the LI Voltage signal of 10 kV peak was generated from the impulse generator and, applied to the transformer through the attenuator circuit. The loading effects of the attenuator distorted its shape and reduced peak magnitude of the impulse injected (at 1U terminal of the transformer). The Injected impulse was with a peak magnitude of 470 V, with its frequency contents spanning from 100 Hz to 10 MHz, which are sufficient for conducting the FRA investigation. Thus, all the requirements of Online IFRA on 315 kVA transformers were successfully met.

Experimental works were done on both the transformers, by following the same procedure under the different load conditions. The respective end-to-end Voltage data were obtained and the transfer function plots were developed. To ensure the repeatability and the reliability of the results, experiments were repeated five times for each case. The average FRA data and the plot for the five sets were obtained and used, as the final representative of the case.

B. PROCEDURE FOLLOWED FOR ANALYSIS

Analysis of the results was done in two steps: In the first step, the comparisons were made between the EEV TF plots of two different cases. Differences between the two compared cases were analyzed by closely observing the changes in the location and magnitudes of spikes and dips. Such changes were utilized as indicators to distinguish one case from another case.

As per literature, the difficulties in interpretations of the FRA results were found to reduce, when they were analyzed through the statistical feature extraction, on the sub-band basis [20]–[22].

Hence, in the second step, a statistical analysis was carried out on the sub-band basis, by extracting the difference between two cases in the form of statistical parameters: Difference Absolute (or) Absolute Difference (DABS), Min-Max ratio (MM ratio (absolute)) and Comparative Standard Deviation (CSD). Details on their calculation procedure are briefed below [20]–[22], [31], [32].

(1) Absolute average Difference (DABS)

$$DABS_{(X,Y)} = \frac{\sum_{i=1}^{N} |Y(i) - X(i)|}{N} \tag{1}$$

where, Xi, Yi are the values in two sets of data and N is the no. of samples in the set. The typical value for (a complete match between the two cases compared) is '0'.This parameter is sensitive to minor differences between the data sets. It gives the average value of deviations.

(2) Minimum-Maximum Ratio (MM absolute)

$$MM = \frac{\sum_{i=1}^{N} min\left(|x_i|, |y_i|\right)}{\sum_{i=1}^{N} max\left(|x_i|, |y_i|\right)} \tag{2}$$

where $|x_i|$ and $|y_i|$ are absolute values of data in two sets and N is the no. of samples in a set.

The typical value is 1. MM is less receptive to changes in the shapes of spikes with a little change in their amplitudes. It considers only maximum and minimum values for each pair of data points.

(3) Comparative Standard Deviation (C.S.D.)

$$CSD(X, Y) = \sqrt{\frac{\sum_{i=1}^{N} \left[\left(\left(X_i - \bar{X}\right) - \left(Y_i - \bar{Y}\right)\right)^2\right]}{N - 1}} \tag{3}$$

where Xi, Yi are the values in two sets of data, $\bar{X}$ and $\bar{Y}$ are their mean values, and N is the no. of samples in a set. The typical value for a complete match between the two datasets is '0'. Here, the variation of each data point with respect to its mean is calculated and used to compute the comparative deviation.

Any deviation of these parameters from their expected typical values is indicative of the difference between the two cases compared. Higher the deviation of the parameter from its typical value, higher will be the difference between the two cases compared. The corresponding frequency sub-band will be considered as the most sensitive frequency range (out of the total frequency spectrum) used in the investigations.

Different statistical parameters were found to offer different sensitiveness, and hence researchers preferred the statistical analysis based on more than one statistical tool. Moreover, different researchers preferred dividing the total frequency spectrum into different sub-band sets, and there are no standard guidelines [20]–[22].

III. RESULTS AND DISCUSSION

For analyzing the effects of the load current magnitudes and its power factor on the diagnosing capability of IFRA, the results of the investigations are compared in the frequency domain, first, with the help of the EEV TF plots and, then, with the help of three statistical parameters DABS, MM ratio (Absolute) and CSD.

Table 1 shows the details of the various healthy cases and the faulty cases investigated in the 5 kVA transformer. The focus was on the effect of the power factor of the load. Throughout the investigation, the total load current was maintained at 4 A and, three power factors (PF) were considered (UPF, 0.5 PF lagging and 0.5 PF leading). The fault was emulated by shorting the (0 V) tapping and the (30 V) tapping of R phase winding of the star side through a 500 Ω, 25 W resistor.

TABLE 1. Investigations of 5 kVA transformer at 4 A load.

Condition of the transformer	Details of the load connected on the transformer	Notation
Healthier Case (HC)	R load, UPF	HC_R
	RL load, 0.5 PF lagging	HC_RL
	RC load, 0.5 PF leading	HC_RC
Faulty case (Sh1)	R load, UPF	Sh1_R
	RL load, 0.5 PF lagging	Sh1_ RL
	RC load, 0.5 PF leading	Sh1_ RC

A. EEV TF PLOTS

The transfer function plot of the healthy case is usually referred to as the signature plot of the transformer [12]–[14]. Figure 7 shows the EEV TF plots of the transformer under its Healthy condition supplying power to the R, RL and RC loads at 4A current levels. They are the signature plots of the transformer, for the three different loads.

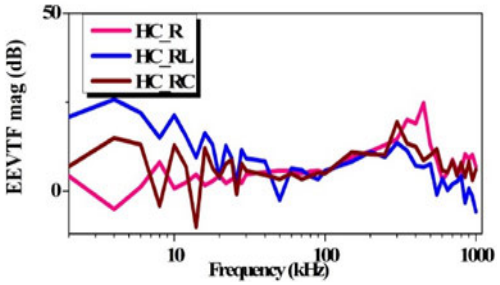

FIGURE 7. Comparison between the EEV TF plots of Healthy Cases at 4 A: with R, RL and RC loads.

In Figure 7, throughout the entire frequency range, there are a lot of differences between the transfer function magnitudes (dB) of the three cases. This indicates that the frequency response of the transformer, even under its healthy condition, is getting influenced by the transformer's load. Therefore, the transfer function plot at one particular load level cannot be considered, directly, as the 'common signature plot' or 'reference plot' of the transformer, for its entire load range.

Figure 8 compares the EEV TF plots of the transformer at a load of 4A under faulty condition with their corresponding healthy cases, for (a) R load (b) RL load and (c) RC load.

There are variations at different frequency ranges, between the EEV TF magnitudes of the Faulty case and the corresponding healthy cases. This indicates that the fault is easily distinguishable from the healthier cases. As the healthy case plots are different for the different types of loads, the variations offered by the fault are also reaching different levels, based on the PF of the loads. This demonstrates the influence of the PF of the load. Therefore, for diagnosing any suspected inter-turn short circuit within a loaded transformer, the healthy case transfer function plot at the corresponding load should be carefully considered as the signature plot.

The lagging and leading PF loads with the same load current magnitude of (4A), the EEV TF plots for same faulty case (Sh1) was varying from their healthy cases to different extents

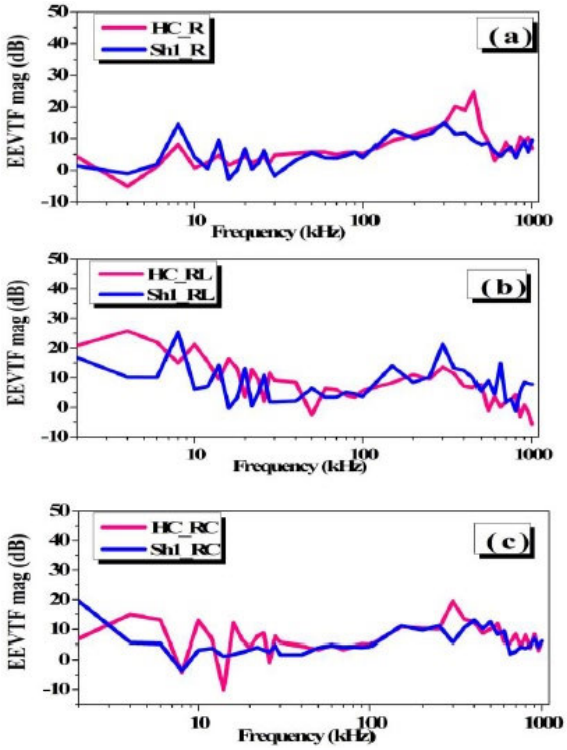

FIGURE 8. Comparison between the EEV TF plots of Healthy and faulty cases at 4A: (a) R load (b) RL load (c) RC load.

and thus, demonstrated that the load power factors have their effects on the frequency response of the transformer. Careful consideration of the transformer's load parameters is, therefore, necessary for the reliable interpretation of the FRA results.

B. STATISTICAL PARAMETERS

Details on the significance of the statistical parameter based comparisons are, explained in detail in the methodology section [20]–[22]. In this approach, comparisons are made between two cases at a time. Deviation of the statistical parametric value from its expected typical value is indicating the difference between the two cases compared [20]. If the deviation is higher at a particular sub-band frequency, it was considered as the highly sensitive sub-band frequency range.

Table 2 shows the statistical comparison of the frequency response of the faulty case (Sh1) at different PF, with the corresponding healthier cases, at the load current level (4 A). The purpose is to analyze the role of the power factor on diagnosing the fault.

The highlighted statistical values correspond to the maximum difference detected for the statistical parameters from their typical values. Higher the difference between the two cases compared, higher will be the deviation of the statistical parameter from its typical value. The corresponding frequency sub-band refers to a frequency range, which offers the most sensitivity to the detection of the difference between the cases. It is observed from Table 3 that, the statistical

TABLE 2. Statistical comparisons for the 5 kVA transformer; Healthier case vs faulty case -at different PF.

Frequency Band kHz	HC_R _vs_ Sh1_R	HC_RL _vs_ Sh1_RL	HC_RC _vs_ Sh1_RC
DABS			
2 - 30	3.07	9.91	5.9
30 -300	1.65	4.08	2.17
300 – 1000	3.75	6.08	6.08
MM(Abs)			
2 - 30	0.46	0.39	5.9
30 -300	0.83	0.60	2.17
300 – 1000	0.67	0.50	6.08
CSD			
2 - 30	5.73	8.82	8.98
30 -300	2.08	4.96	4.34
300 – 1000	4.69	5.65	5.65

parameters vary to a different extent at different sub-bands and, in detecting the same fault, offer different sensitivity at different PF. This demonstrates again that the IFRA approach on the loaded transformer is sensitive to its load power factor.

Hence, the effect of loads connected to the transformer needs to be carefully considered, when the Online FRA approach is implemented for the diagnosis of faults within the transformer.

In the case of the second transformer (315 kVA), the work was split into two parts, with the focus gradually being increased in two steps;

TABLE 3. Investigations of 315 kVA transformer at 10 A load.

Condition of the transformer	Details of the load connected on the transformer	Notation
Healthier Case (HC)	R load, U.P.F	HC_R_10A
	RL load, 0.94 PF lagging	HC_ RL_ 10A
	RC load, 0.94 PF leading	HC_ RC_ 10A
Faulty case-1 (FC 1)	R load, U.P.F	FC1_R_10A
	RL load, 0.94 PF lagging	FC1_RL_ 10A
	RC load, 0.94 PF leading	FC1_RC_ 10A
Faulty case-2 (FC 2)	R load, U.P.F	FC2_R_10A
	RL load, 0.94 PF lagging	FC2_RL_ 10A
	RC load, 0.94 PF leading	FC2_RC_ 10A

In the first step, the focus was on the usefulness of IFRA technique in discriminating between the two faults of the same level, but, at different locations. The experiments were done at a total load current of 10 A level at UPF, 0.94 PF lagging and 0.94 PF leading. The frequency response of the transformer in the healthy and faulty condition was observed. In this case, the inter-turn shorts were emulated by shorting the special tappings of R phase winding of the delta side through a 245 Ohm resistor. Two such shorts of the same level, but, at different locations, were emulated (only one at a time): (1) Faulty case-1 (FC1), by shorting the (1U) and 87.5% tappings (i.e. tappings t1 and t2) and, ((2) Faulty case-2 (FC2) by shorting the 12.5 % and (1V) tappings (i.e. tappings t5 and t6). Table 3 shows the details of the various healthy cases and the faulty cases investigated in the 315 kVA transformer at 10 A load level.

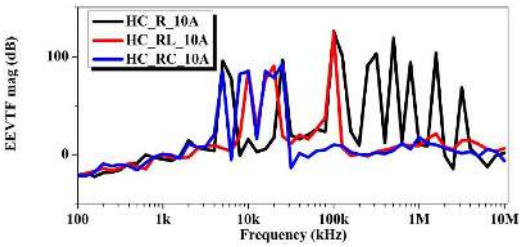

FIGURE 9. Comparison between the Healthy case EEV TF plots of at 10 A: with R, RL and RC loads.

Figure 9 shows the EEV TF plots of the transformer under its Healthy condition supplying power to the R, RL and RC loads at 10A current levels. They are the signature plots of the transformer for the three different loads.

Variations observed between the healthier case plots at different PF, again, demonstrates the influence of the power factor on the frequency response of the transformer.

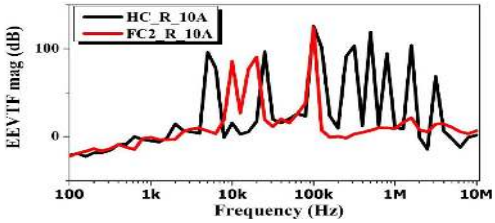

FIGURE 10. Comparison between the Healthy case and the faulty case plots of the transformer with a resistive load of 10 A.

Figure 10 shows the EEV TF plots of healthy and the Faulty case, with the 10 A, resistive (UPF) load alone. Here, the plot of the healthy case is compared with the plots of the Faulty cases (FC1 and FC 2). The purpose is to assess the capability of IFRA in discriminating between the locations of the fault when the transformer is On-load.

It can be noted that the faults are of the same level (short of 12.5 % of the winding), but, at a different location, FC1 being near to the impulsed end (1U) and FC2 being near to the non impulsed end (1V). The Plots of the two faulty cases vary distinctly from the plot of the healthy case, demonstrating the usefulness of the IFRA in discriminating between the two faults of the same level, but, at different locations.

For investigating the influence of the power factor of the load on the fault discrimination capability of IFRA, further investigations are done with the RL and RC loads. Figure 10 shows the EEV TF plots of healthy and the Faulty cases, with the 10 A, RL (0.94 lagging) and RC (0.94 leading) loads.

The Plots of the two faulty cases vary distinctly from the plots of the respective healthy cases. It can be noted that both the RL and the RC loads have the same load current magnitudes and, their power factor (PF) alone is different. For both the RL and the RC loads, the Plots of the two faulty cases (FC1 and FC2) vary distinctly from the plot of the respective

healthy cases. For analyzing the influence of PF of the load in discriminating between the two faults, a cross-comparison is made between Figures 10 (a) and 10 (b). Variations are found throughout the frequency spectrum and, reveals that the faulty case variations from their respective healthier case plots are considerably distinct. Thus, the cross comparison, additionally demonstrates that the signature plots at appropriate power factors have to be preferred in carefully capitalizing the usefulness of the IFRA in discriminating between the location of the fault.

Table 4 shows the statistical comparison of the frequency response of the faulty cases (FC1) and (FC2) with the healthier case, when the transformer is supplying a resistive load of (10 A). The purpose is to analyze the usefulness of IFRA in discriminating between the locations of the Fault. For a simpler representation, the healthier case corresponding to the resistive load of 10 A (HC-R_10A) is referred in the table 4 as, HC_R.

TABLE 4. Statistical comparisons for the 315 kVA transformer; Healthier case vs faulty case -at 10 A, resistive load.

Frequency sub-band (kHz)	HC_R Vs FC1	HC_R Vs FC2
DABS		
30	41.31	35.64
30 -300	32.18	49.28
300-1000	51.32	54.15
MM(Abs)		
2-30	0.16	0.39
30 -300	0.40	0.09
300-1000	0.12	0.10
CSD		
2-30	52.95	46.19
30 -300	42.07	39.27
300-1000	48.30	50.92

As seen from Table 4, for the two faults of the same level, but, at different location the statistical values DABS, MM (Abs) and CSD differ from their typical values to different extents in all the three sub-bands. Thus, IFRA is also found useful in discriminating between the locations of the faults.

Table 5 shows the statistical comparison of the frequency response of the faulty cases (FC1) and (FC2) with the healthier case, when the transformer is supplying RL and RC loads (10 A, 0.94 lagging and leading). The purpose is to analyze the influence of the PF, on the location discrimination. For a simpler representation, the healthier case corresponding to the RL and RC loads of 10 A (HC_RL_10A and HC_RC_10A) is referred in the table 5 as, (HC_RL) and (HC_RC), respectively.

As seen from Table 5, the statistical values DABS, MM (Abs) and CSD differ from their typical values to different extents in all the three sub-bands. Moreover, when the PF is changed from lagging to leading, these statistical values are changing. Thus the PF of the load is found to influence the sensitivity of IFRA in diagnosing and discriminating between

TABLE 5. Statistical comparisons for the 315 kVA transformer; Healthier case vs faulty case -at 10 A, RL and RC loads.

Frequency sub-band (kHz)	RL load		RC load	
	HC_RL vs FC1	HC_RL vs FC2	HC_RC vs FC1	HC_RC vs FC2
DABS				
2-30	12.20	15.23	30.35	29.31
30 -300	25.61	41.73	42.45	40.36
300-1000	14.02	17.01	3.47	53.53
MM(Abs)				
2-30	0.34	0.38	0.28	0.38
30 -300	0.44	0.08	0.17	0.30
300-1000	0.34	0.35	0.65	0.12
CSD				
2-30	20.52	23.13	45.08	42.73
30 -300	33.18	44.72	50.50	37.70
300-1000	5.21	10.54	5.16	48.62

the faults. Based on the PF of the load, a careful comparison is needed between the corresponding signature response and the faulty case response.

In the second step of investigation on the 315 kVA transformer, the focus was further extended. Investigations were done to assess the usefulness of IFRA technique in discriminating between the faults of the same and different severity levels, at different locations. The experiments were done at a total load current of 11 A level at UPF, 0.85 PF lagging and 0.85 PF leading. The frequency responses of the transformer in the healthy and faulty condition were observed. Three different faulty cases were emulated, at three different positions (only one fault was considered at a time).

The first two cases were of equal severity level, but, at different locations within the winding; (1) Faulty case-1 (FC1), by shorting the tappings t1 and t2 (i.e. shorting 12.5% of the winding near the terminal (1U)) (2) Faulty case-2 (FC2) by shorting the tappings t5 and t6 (i.e. shorting 12.5% of the winding near the terminal (1V)). The third case (Faulty case-3 (FC3)) was for a different severity level and, emulated by shorting the tappings t2 and t3 (i.e. shorting 25% of the winding near the terminal (1U)).

Table 6 shows the details of the various healthy cases and the faulty cases investigated in the 315 kVA transformer at 11 A load level.

Figure 12 shows the EEV TF plots of the transformer under its healthy condition supplying power to the resistive load at two different current levels (10A and 11 A). Variations are observed between these signature plots of two healthy cases at the two current levels, but, at the same power factor (Unity). This indicates that the load magnitude can influence the signature frequency response pattern.

Figure 13 shows the EEV TF plots of the transformer under its healthy condition supplying power to the R, RL and RC loads at 11A current levels.

In Figure 13, variations are observed between the healthier case plots at different PF at this new current level of 11 A.

TABLE 6. Investigations of 315 kVA transformer at 11 A load.

Condition of the transformer	Details of the load connected on the transformer	Notation
Healthier Case (HC)	R load, U.P.F	HC_R_11A
	RL load, 0.85 PF lagging	HC_ RL_ 11A
	RC load, 0.85 PF leading	HC_ RC_ 11A
Faulty case-1 (FC 1)	R load, U.P.F	FC1_R_11A
	RL load, 0.94 PF lagging	FC1_ RL_ 11A
	RC load, 0.94 PF leading	FC1_ RC_ 11A
Faulty case-2 (FC 2)	R load, U.P.F	FC2_R_11A
	RL load, 0.94 PF lagging	FC2_ RL_ 11A
	RC load, 0.94 PF leading	FC2_ RC_ 11A
Faulty case-3 (FC 3)	R load, U.P.F	FC3_R_11A
	RL load, 0.94 PF lagging	FC3_ RL_ 11A
	RC load, 0.94 PF leading	FC3_ RC_ 11A

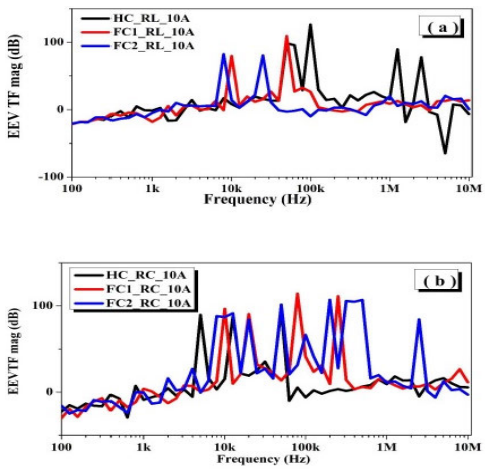

FIGURE 11. Comparison between the Healthy and the Faulty case EEV TF plots at 10 A: with RL and RC loads.

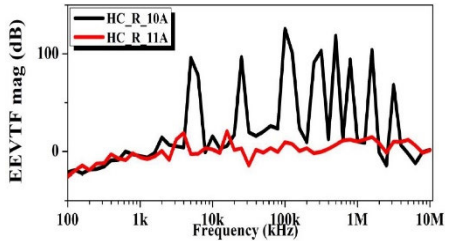

FIGURE 12. Comparison between the Healthy case EEV TF plots of transformer with resistive loads of 10 A and 11 A.

This is again confirming that effect of the power factor on the frequency response of the transformer can alter the signature plot.

Further comparisons were made between the healthy case and the faulty case with the RL and the RC loads at 11 A level; at 0.94 PF lagging and 0.94 PF leading. Figure 13 shows the EEV TF plots of the transformer with the 11 A, at the lagging and the leading PF loads. The focus was on the usefulness of the IFRA in discriminating between the fault location and fault severity levels. FC1 and FC2 are the faults of the

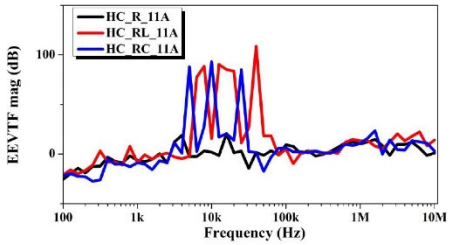

FIGURE 13. Comparison between the Healthy case and the faulty case plots of transformer with a resistive load of 11 A.

same level (12.5% short), but, at different location. FC3 (25% short) is more severe than FC1 and FC2.

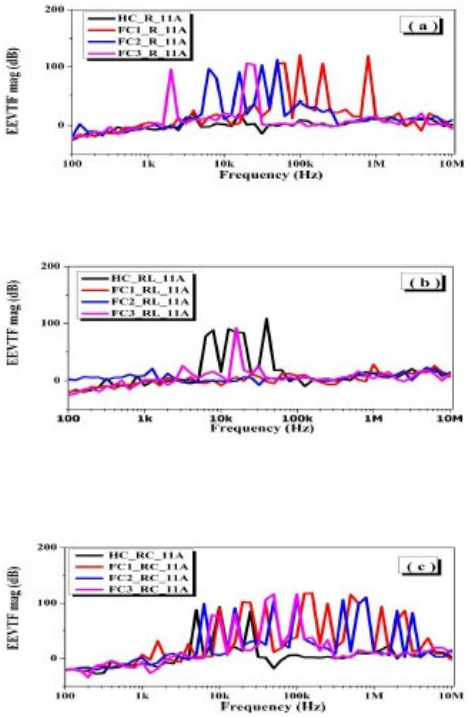

FIGURE 14. Comparison between the Healthy and the Faulty case EEV TF plots of transformer at 11 A- with RL and RC loads.

From Figure 14, the following observations are made; (1) All the faulty case plots of the R, RL and RC loads are deviating from their respective healthy case plots and thus demonstrates the usefulness of IFRA in diagnosing the inter-turn shorts. (2) Deviations between the FC1 and FC2 plots in all the sub figures (14. a, b and c) indicates that the two faults of the same level, but, at different locations can be distinguished through the IFRA approach. (3) Deviations of The plot (FC3) from the other two faulty case plots (FC1 and FC2) indicate that the faults of different severity level can also be effectively distinguished through the IFRA approach.

To ascertain the above findings, different cases are also compared through the statistical parameters. Table 7 shows the comparisons made between the healthy case and the three

faulty cases of the 315 kVA transformer when it supplies power to 11 A, resistive load. Here, in columns 2 and 3, the focus is on the usefulness of IFRA in discriminating within the fault locations. In column 4, to assess the usefulness of IFRA in discriminating within the severity levels of the faults, a more severe fault (25 % short) is compared with the healthy case plot. For a simpler representation, the healthier case corresponding to the resistive load of 11 A (HC-R_11A) is referred in the table 7 as (HC_R).

TABLE 7. Statistical comparisons for the 315 kVA transformer; Healthier case vs faulty case - at 11 A, resistive load.

Frequency sub-band (kHz)	R load 11 A HC_R vs FC1	HC_R vs FC2	HC_R vs FC3
	DABS		
2-30	15.64	37.28	33.18
30 -300	53.55	40.01	4.26
300-1000	28.16	2.97	2.66
	MM(Abs)		
2-30	0.30	0.15	0.12
30 -300	0.08	0.10	0.35
300-1000	0.20	0.67	0.71
	CSD		
2-30	15.07	39.66	39.90
30 -300	39.54	36.59	6.25
300-1000	36.25	3.44	2.73

In the table 7, the maximum deviations of the statistical parameters from their typical values are highlighted. The corresponding frequency band offers high sensitivity in discriminating the faulty case from the healthy case. In this table, columns 2 and 3 compare the two same level faults (12.5% shorts) with the healthier case and, column 4 compares the more severe fault (25% short) with the healthier case. It is evident from the table that for different faults, these maximum deviations occur either at different frequency bands or, atleast their numerical values are numerically different when they happen to occur at the same frequency band. The differences observed between the columns 2 and 3 of table confirm the usefulness of IFRA in discriminating between the faults at different locations. The difference observed between the column-4 and the column-2 or 3, confirm the usefulness of IFRA in discriminating between two faults of different severity levels.

Table 8 shows the comparisons made between the healthy case and the three faulty cases of the 315 kVA transformer when it supplies power to, RL and RC loads (11 A, 0.85 PF lagging and leading). Here, two loads of same current magnitude, but of different power factor (0.85 lagging for RL load and 0.85 leading for the RC load) are considered. The focus is given to the influence of the PF on the fault discriminating capability IFRA. For a simpler representation, the healthier case corresponding to the RL and RC loads of 11 A (HC_RL_11A and HC_RC_11A) is referred in the table 5 as (HC_RL) and (HC_RC), respectively

TABLE 8. Statistical comparisons for the 315 kVA transformer; Healthier case vs faulty case -at 11 A, RL and RC loads.

Frequency sub-band (kHz)	RL load 11 A HC_RL vs FC1	HC_RL vs FC2	HC_RL vs FC3	RC load 11 A HC_RC vs FC1	HC_RC vs FC2	HC_RC vs FC3
			DABS			
2-30	37.29	38.77	28.79	24.55	38.45	26.40
30 -300	19.81	17.99	15.62	54.84	38.32	49.73
300-1000	9.56	2.88	4.98	58.18	51.90	2.89
			MM (Abs)			
2-30	0.10	0.06	0.35	0.44	0.20	0.35
30 -300	0.22	0.17	0.24	0.07	0.11	0.08
300-1000	0.26	0.67	0.49	0.09	0.10	0.67
			CSD			
2-30	40.59	40.83	38.01	36.98	50.62	39.13
30 -300	33.13	30.86	31.56	38.74	35.76	42.63
300-1000	10.78	3.72	5.55	43.16	46.90	2.79

In the table 8, the maximum deviations of the statistical parameters from their typical values are highlighted. The corresponding frequency band offers high sensitivity in discriminating the faulty case from the healthy case. In this table, columns 2, 3, 5 and 6 compare the two same level faults (12.5% shorts) with the healthier case and, columns 4 and 6 compares the more severe fault (25% short) with the healthier cases. It is evident from the table that for different faults, these maximum deviations occur either at different frequency bands or, atleast their numerical values are different when they happen to occur at the same frequency band. The differences observed between the columns 2 and 3 of the table confirm the usefulness of IFRA in discriminating between the faults at different locations. The difference observed between the column-4 and the column-2 or 3, confirm the usefulness of IFRA in discriminating between two faults of different severity levels.

In consolidation, the above investigations on the 5 kVA and 315 kVA transformers confirms that IFRA Online implementation is more challenging than the conventional Off-line FRA, as, both the load current magnitude and PF can influence the IFRA results. However, the results obtained through the careful comparison of the various faulty cases with their corresponding healthy cases revealed that, IFRA online can be successfully implemented at different current magnitudes and PF, for diagnosing the inter-turn shorts and discriminating within different inter-turn shorts.

IV. CONCLUSION

Experimental investigations were carried out on a three phase 5 kVA, 440 V/440 V Star/Delta transformers and a three phase 315 kVA, 11 kV/ 433 V, Dyn11 distribution transformer, when they were was supplying power to loads of different magnitudes and power factors.

IFRA results of the transformer with the EEV TF approach were observed for the transformer for the healthy condition and with the emulated inter-turn shorts in one of the windings.

Comparisons made between the IFRA results of the transformer, under different loads revealed that both the magnitude

of the load current and its power factor can influence the frequency response of the transformer. The healthy case frequency responses (signature plots) were found to be different under different loads and thus, revealed that the signature plots developed for a particular load level cannot be considered directly as a common representative FRA signature of the transformer for its entire permissible load range. The difference between the frequency response of the healthy case and the faulty case was also found to vary to different extents for different load currents and power factors. Comparisons made between the various healthy and faulty cases in terms of the EEV TF plots and the statistical parameters showed that there were a lot of variations in the frequency responses. However, for different faults, the magnitudes of the statistical variations with reference to their corresponding signature plots were found to be distinct at different sub-bands. Thus, IFRA was found to be effective in discriminating between the locations as well as severity levels of faults

The variations in the statistical parameters were also found to be the maximum at certain frequency sub-bands; At these sub-bands, IFRA was found to offer maximum sensitivity in diagnosis. More attention has to be paid in these frequency ranges during IFRA based inter-turn diagnosis of loaded transformers.

The results become significant as they are reported first-time and demonstrated that both the load magnitudes and the power factor can severely influence the frequency response of the transformer and can alter the sub-band sensitivity of the IFRA based diagnostic process.

For generalizing the findings, further research works can be done in future, on bigger transformers of different winding types and other types of faults with different severity levels.

ACKNOWLEDGMENT

The authors thank S. Mohamad Ghouse and J. Rajamohan of SASTRA for helping in the preparation of the manuscript.

REFERENCES

[1] S. Tenbohlen, D. Uhde, J. Poittevin, H. Borsi, P. Werle, U. Sundermann, and H. Matthes, "Enhanced diagnosis of power transformers using on- and off-line methods: Results, examples and future trends," in *Proc. Cigré Session*, Mar. 2000, Paper 12-204.

[2] S. Tenbohlen, S. Coenen, M. Djamali, A. Müller, M. Samimi, and M. Siegel, "Diagnostic measurements for power transformers," *Energies*, vol. 9, no. 5, p. 347, May 2016.

[3] S. Alsuhaibani, Y. Khan, A. Beroual, and N. Malik, "A review of frequency response analysis methods for power transformer diagnostics," *Energies*, vol. 9, no. 11, p. 879, Oct. 2016.

[4] R. Malewski and B. Poulin, "Impulse testing of power transformers using the transfer function method," *IEEE Trans. Power Del.*, vol. 3, no. 2, pp. 476–489, Apr. 1988.

[5] M. Wang, A. J. Vandermaar, and K. D. Srivastava, "Transformer winding movement monitoring in service–key factors affecting FRA measurements," *IEEE Elect. Insul. Mag.*, vol. 20, no. 5, pp. 5–12, Sep./Oct. 2004.

[6] A. Abu-Siada, N. Hashemnia, S. Islam, and M. Masoum, "Understanding power transformer frequency response analysis signatures," *IEEE Elect. Insul. Mag.*, vol. 29, no. 3, pp. 48–56, May 2013.

[7] E. Al Murawwi, R. Mardiana, and C. Q. Su, "Effects of terminal connections on sweep frequency response analysis of transformers," *IEEE Elect. Insul. Mag.*, vol. 28, no. 3, pp. 8–13, May 2012.

[8] A. Srikanta Murthy, N. Azis, S. Al-Ameri, M. Mohd Yousof, J. Jasni, and M. Talib, "Investigation of the effect of winding clamping structure on frequency response signature of 11 kV distribution transformer," *Energies*, vol. 11, no. 9, p. 2307, Sep. 2018.

[9] J. Jayasinghe, Z. D. Wang, P. N. Jarman, and A. W. Darwin, "Winding movement in power transformers: A comparison of FRA measurement connection methods," *IEEE Trans. Dielectr. Elect. Insul.*, vol. 13, no. 6, pp. 1342–1349, Dec. 2006.

[10] S. A. Ryder, "Diagnosing transformer faults using frequency response analysis," *IEEE Elect. Insul. Mag.*, vol. 19, no. 2, pp. 16–22, Mar. 2003.

[11] Q. Yang, P. Su, and Y. Chen, "Comparison of impulse wave and sweep frequency response analysis methods for diagnosis of transformer winding faults," *Energies*, vol. 10, no. 4, p. 431, Mar. 2017.

[12] *Mechanical Condition Assessment of Transformer Windings Using Frequency Response Analysis (FRA)*, document C.I.G.R.E. WG A2.26, Paris, France, 2008.

[13] *IEEE Guide for the Application and Interpretation of Frequency Response Analysis for Oil-Immersed Transformers*, IEEE Standard C57.149, New York, NY, USA, 2012.

[14] *Measurement of Frequency Response*, Edition 1.0, IEC Standard 60076-18, 2012.

[15] J. Liu, Z. Zhao, C. Tang, C. Yao, C. Li, and S. Islam, "Classifying transformer winding deformation fault types and degrees using FRA based on support vector machine," *IEEE Access*, vol. 7, pp. 112494–112504, 2019.

[16] E. Gomez-Luna, G. A. Mayor, and J. P. Guerra, "Application of wavelet transform to obtain the frequency response of a transformer from transient signals—Part II: Practical assessment and validation," *IEEE Trans. Power Del.*, vol. 29, no. 5, pp. 2231–2238, Oct. 2014.

[17] Z. Zhao, C. Tang, Q. Zhou, L. Xu, Y. Gui, and C. Yao, "Identification of power transformer winding mechanical fault types based on online IFRA by support vector machine," *Energies*, vol. 10, no. 12, p. 2022, 2017.

[18] Z. Zhao, C. Tang, C. Yao, Q. Zhou, L. Xu, Y. Gui, and S. Islam, "Improved method to obtain the online impulse frequency response signature of a power transformer by multi scale complex CWT," *IEEE Access*, vol. 6, pp. 48934–48945, 2018.

[19] V. Nurmanova, M. Bagheri, A. Zollanvari, K. Aliakhmet, Y. Akhmetov, and G. Gharehpetian, "A new transformer FRA measurement technique to reach smart interpretation for inter-disk faults," *IEEE Trans. Power Del.*, vol. 34, no. 4, pp. 1508–1519, Aug. 2019.

[20] W. C. Sant'Ana, C. P. Salomon, G. Lambert-Torres, L. E. Borges da Silva, E. L. Bonaldi, L. E. de Lacerda de Oliveira, and J. G. Borges da Silva, "A survey on statistical indexes applied on frequency response analysis of electric machinery and a trend based approach for more reliable results," *Electr. Power Syst. Res.*, vol. 137, pp. 26–33, Aug. 2016.

[21] K. P. Badgujar, M. Maoyafikuddin, and S. V. Kulkarni, "Alternative statistical techniques for aiding SFRA diagnostics in transformers," *IET Gener., Transmiss. Distrib.*, vol. 6, no. 3, pp. 189–198, 2012.

[22] V. Behjat and M. Mahvi, "Statistical approach for interpretation of power transformers frequency response analysis results," *IET Sci., Meas. Technol.*, vol. 9, no. 3, pp. 367–375, May 2015.

[23] A. A. Devadiga, N. Harid, H. Griffiths, N. Al Sayari, B. Barkat, S. Jayaram, and Y. Taniguchi, "Winding turn-to-turn short-circuit diagnosis using FRA method: Sensitivity of measurement configuration," *IET Sci., Meas. Technol.*, vol. 13, no. 1, pp. 17–24, 2018.

[24] R. Rajamani, M. Rajappa, and B. Madanmohan, "Sweep frequency response analysis based diagnosis of shorts within transformer windings," *IET Gener., Transmiss. Distrib.*, vol. 11, no. 17, pp. 4274–4281, Nov. 2017.

[25] V. Behjat, A. Vahedi, A. Setayeshmehr, H. Borsi, and E. Gockenbach, "Sweep frequency response analysis for diagnosis of low level short circuit faults on the windings of power transformers: An experimental study," *Int. J. Electr. Power Energy Syst.*, vol. 42, no. 1, pp. 78–90, Nov. 2012.

[26] E. Gomez-Luna, G. Aponte Mayor, C. Gonzalez-Garcia, and J. Pleite Guerra, "Current status and future trends in frequency-response analysis with a transformer in service," *IEEE Trans. Power Del.*, vol. 28, no. 2, pp. 1024–1031, Apr. 2013.

[27] M. Bagheri, M. S. Naderi, and T. Blackburn, "Advanced transformer winding deformation diagnosis: Moving from off-line to on-line," *IEEE Trans. Dielectr. Elect. Insul.*, vol. 19, no. 6, pp. 1860–1870, Dec. 2012.

[28] V. Behjat, A. Vahedi, A. Setayeshmehr, H. Borsi, and E. Gockenbach, "Diagnosing shorted turns on the windings of power transformers based upon online FRA using capacitive and inductive couplings," *IEEE Trans. Power Del.*, vol. 26, no. 4, pp. 2123–2133, Oct. 2011.

[29] T. De Rybel, A. Singh, J. A. Vandermaar, M. Wang, J. R. Marti, and K. D. Srivastava, "Apparatus for online power transformer winding monitoring using bushing tap injection," *IEEE Trans. Power Del.*, vol. 24, no. 3, pp. 996–1003, Jul. 2009.
[30] M. Bagheri, S. Nezhivenko, and B. T. Phung, "Loss of low-frequency data in on-line frequency response analysis of transformers," *IEEE Elect. Insul. Mag.*, vol. 33, no. 5, pp. 32–39, Sep./Oct. 2017.
[31] R. Rajamani, M. Rajappa, K. Arunachalam, and B. Madanmohan, "Inter-turn short diagnosis in small transformers through impulse injection: On-line on-load self-impedance transfer function approach," *IET Sci., Meas. Technol.*, vol. 11, no. 8, pp. 961–966, 2017.
[32] N. Shanmugam, B. Madanmohan, and R. Rajamani, "Influence of the load on the impulse frequency response approach based diagnosis of transformer's inter-turn short-circuit," *IEEE Access*, vol. 8, pp. 39454–39463, 2020.
[33] *Datasheet*, Manual of Keysight Iniiivision DSOX1102G, Keysight, Santa Rosa, CA, USA, 2018.

NATARAJAN SHANMUGAM is currently pursuing the Ph.D. degree with Shanmugha Arts, Science, Technology and Research Academy (SASTRA) Deemed University, Thanjavur, India. His current research interests include high voltage testing, condition assessment, and fault diagnosis in electrical equipment.

SRINIVASAN GOPAL was born in Chennai, in June 1946. He is currently pursuing the Ph.D. degree in high voltage engineering from IIT Madras. His professional experience spans over a period of about 40 years—about half of which in teaching and research at IIT, Madras. From 1973 to 1974, he was deputed to Germany on Indo-German Scholarship for advanced training in high voltage engineering. He was associated with the NBA Team of AICTE, as an Expert, for Accreditation of Engineering Colleges. He also served as a Reporter in the prestigious International Symposium on High Voltage Engineering (ISH 2001) held at Bangaluru. Since 1984, he has been heading W.S. Test Systems Private Ltd., (formerly known as MWB (India) Ltd.), where he is engaged in the manufacture of high voltage test and measuring equipment. He is actively engaged in the academic activities and is currently a AICTE Distinguished Visiting Professor of high voltage engineering with Shanmugha Arts, Science, Technology and Research Academy (SASTRA) University, Thanjavur, and also a member of the Research Advisory Committee, Vellore Institute of Technology, Vellore. He is also a member of BIS for High Voltage Test Techniques and WG 33-03 of National Study Committee on Digital Techniques in HV Measurement.

BALASUBRAMANIAN MADANMOHAN (Member, IEEE) was born in Tamil Nadu, India, in 1981. He received the bachelor's degree in electrical and electronics engineering from Bharathidasan University, in 2002, and the master's and Ph.D. degrees from Shanmugha Arts, Science, Technology and Research Academy (SASTRA) Deemed University, Thanjavur, India, in 2006 and 2017, respectively. He is currently a Faculty with the School of Electrical and Electronics Engineering, SASTRA Deemed University. His research interests include partial discharge signature analysis, condition assessment of power apparatus, ageing characterization of insulation systems, and frequency response analysis for transformer fault diagnosis. He is an active member of the IEEE Dielectrics and Electrical Insulation Society and the Power and Energy Society.

S. P. BALAJI (Member, IEEE) received the bachelor's, master's, and Ph.D. degrees in 2006, 2008, and 2016, respectively. He is currently with GPRI, India, and is actively contributing in academic and industry.

RAJESH RAJAMANI received the Ph.D. degree from Shanmugha Arts, Science, Technology and Research Academy (SASTRA) Deemed University, Thanjavur, India, in 2018. He is currently working as an Assistant Professor with the Department of Electrical and Electronics Engineering, SASTRA. His current research interests include high voltage testing, condition monitoring, and fault diagnosis.